

# **Integration of CBCT and a Skull Base Drilling Robot**

Computer Integrated Surgery II, Spring, 2011

Hao Dang and Zihan Chen

Mentors: Dr. Jeffrey Siewerdsen and Dr. Peter Kazanzides

**2011-5-19**

# Contents

## **1. Introduction**

- 1.1 Clinical requirements
- 1.2 Image guided robots
- 1.3 Current skull base robot system

## **2. Materials**

- 2.1 C-arm Cone Beam CT imaging device
- 2.2 NeuroMate skull base robot system
- 2.3 Polaris optical tracking system
- 2.4 Imaging and surgical navigation platform—TREK
- 2.5 Phantom

## **3. Methods**

- 3.1 Overview of registration workflow
- 3.2 Technical approach

## **4. Experiments and Results**

- 4.1 Experiment methods
  - 4.1.1 Pre-operative CT to intra-operative CBCT registration
  - 4.1.2 Image to tracker registration
  - 4.1.3 Robot to tracker registration
  - 4.1.4 Virtual Fixture
  - 4.1.5 Real time visualization of cutting tool
  - 4.1.6 Summary of system integration
- 4.2 Experiment results on Red Skull phantom
  - 4.2.1 Pre-operative CT to intra-operative CBCT registration
  - 4.2.2 CT to tracker registration
  - 4.2.3 Robot to tracker registration
- 4.3 Experiment results on foam phantom
  - 4.3.1 A robot tool for ablation
  - 4.3.2 Image to tracker registration
  - 4.3.3 Robot to tracker registration
  - 4.3.4 Target-pointing experiment results
  - 4.3.5 Virtual fixture experiment results

## **5. Management summaries**

- 5.1 Credits
- 5.2 Accomplishment vs. Plan
- 5.3 Future plan

## **6. Technical Appendices**

- 6.1 How to use NDI software ‘Track’
- 6.2 How to install Qt on Windows/Linux
- 6.3 How to use software TREK

# Integration of CBCT and a Skull Base Drilling Robot

Computer Integrated Surgery II, Spring, 2011

Hao Dang and Zihan Chen

Mentors: Dr. Jeffrey Siewerdsen and Dr. Peter Kazanzides

## 1. Introduction

### 1.1 clinical requirements

Neurosurgery (or neurological surgery) is the medical specialty concerned with the prevention, diagnosis, treatment and rehabilitation of disorders that affect any portion of the nervous system including the brain, spinal column, spinal cord, peripheral nerves, and extra-cranial cerebrovascular system [1].

Neurosurgery involves many challenges for traditional surgical procedures.

- (1) First, human head has complex anatomy including complex bony structure and critical adjacent neural and vascular structures [3]. Thus, there is a great need in neurosurgery for high precision information-- knowing exactly where the critical structures are.
- (2) Second, nearly all neurosurgical procedures require some amount of bone cutting—typically a craniotomy or craniectomy. In some cases, it is necessary to do further bone milling inside the skull, often at the skull base, to gain access to a tumor or vascular lesion [2]. However, the skull base is one of the most complex and vulnerable anatomical areas, taking a surgeon as long as six to fifteen hours to work in the operation room. So it will bring the neurosurgeon accumulated fatigue and dexterity if he/she has to always hold the drill and continuously focus.
- (3) Third, once knowing the accurate anatomy and having mechanical support against fatigue and dexterity, a neurosurgeon may still make mistake in drilling if there is a lack of constrain mechanism.



Fig1:[http://www.gammaknifeonline.in/gamma\\_knife\\_for\\_acoustic\\_neuroma](http://www.gammaknifeonline.in/gamma_knife_for_acoustic_neuroma)

For example, when drilling the posterior wall of the internal auditory canal in acoustic neuroma surgery, critical structures such as the semicircular canals, the cochlea, facial nerve and jugular bulb are within millimeters. Even when using an established surgical approach, the surgeon may damage the inner ear, vestibular apparatus, adjacent nerves or jugular bulb [3].

### 1.2 Image guided robots

Computer Integrated Surgery (CIS) is a scientific field that focuses on computer-based techniques, systems, and applications exploiting quantitative information from medical images and sensors to assist clinicians in all phases of treatment [4]. It has been gaining more and more significance in many fields of medicine these days. Most commonly, medical robots have been used for prostatectomy, nephrectomy, cholecystectomy, orthopedics and interventional radiology, where mechatronic devices provide apparent advantages [2].

Robotic systems accompanied by image guidance is capable of providing both 1) mechanical assistance against limits of fatigue and dexterity virtual fixture against outcut and damage of critical structure, 2) and precise intra-operative guidance limits of human vision.

On the other side, neurosurgery itself is well suited to the use of image-guided robots, due to the static nature of the human skull and locally fixed segments of the spine [3].

### 1.3 Current skull base robot system



Fig 2. Current skull base robot system [3]

Current skull base robot system developed in Prof. Peter Kazanzides' lab integrated a Stealthstation navigation system, a NeuroMate robotic arm with a six degree-of-freedom force sensor, and 3D Slicer visualization software to allow the use of the robotic arm in a navigated, cooperatively-controlled fashion by the surgeon. Pre-defined virtual fixture has also been developed to constrain the motion of the robot-held cutting tool within safe zone [3].

The system yielded high accuracy in phantom study--0.6 mm average placement error and 0.6 mm average dimensional error. But in cadaver study some bone outside virtual fixture was cut and the typical overcut was 1–2 mm, with maximum about 3 mm. This keeps the robot from being further tested in real clinical trial.

In the cadaver studies, we notice that the pre-operative registration residual errors were fairly low. For instance, the error for transform between Stealth reference frame to the Stealth CT frame was below 1 mm, and the error for transform between reference frame to the Robot world frame was below 0.5 mm. However, registration error went higher during operation. This raises an interesting question that why the system started with good registration but ended with large outcut. Since the robot drill was operated directly under constrain defined by virtual fixture (VF), a critical reason for the increased error may lie in that the VF was not updated intra-

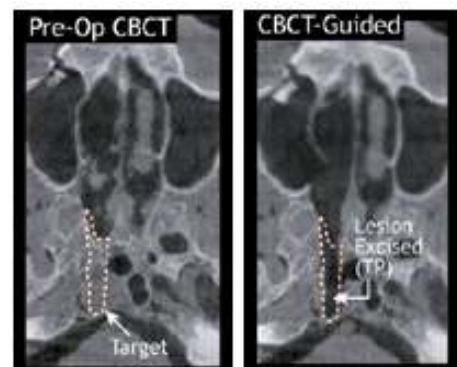


Fig 3: Deformation during surgery [9]

operatively. In other words, VF was defined on pre-operative CT images and transformed to robot world frame by pre-operative registration. However, there are a series of conditions in which

deformation is introduced.

- (1) Drilling and other surgical operations introduced bone drill out and soft tissue deformation, so the pre-operative image information could not match with intra-operative anatomy.
- (2) Undetected patient motion (lack of motion detection or deficiencies in motion detection) may contribute to this error.
- (3) Changes in head pose between CT imaging and surgical operation will also introduce deformation. This could turn out to be a more important issue if the surgery was performed on a patient not only a cadaver head.

#### **1.4 Integration of a C-arm Cone Beam CT imaging system**

Considering that intra-operatively updating anatomical deformation and refining registration of the robotic system may be a possible way to increase cutting accuracy, an advanced intra-operative imaging device--C-arm cone-beam CT (CBCT) will be integrated into the robot system. This prototype CBCT imaging system based on a mobile isocentric C-arm has been developed in Prof. Jeff Siewerdsen's lab in collaboration with Siemens Healthcare (Siemens SP, Erlangen Germany). It has



Fig 4: C-arm Cone Beam CT [10]

demonstrated sub-mm 3D spatial resolution and soft tissue visibility which are suitable for neurosurgery navigation. The typical acquisition and reconstruction time are ~60s and ~20s respectively which will not interrupt the typical surgical workflow. Although imaging dose has tradeoffs with image quality, the dose of CBCT is largely reduced from traditional diagnostic CT.

## **2. Materials**

The proposed system in this project includes several components: C-arm Cone Beam CT imaging device (Siemens SP, Erlangen Germany), NeuroMate skull base robot system (Integrated Surgical Systems, Sacramento, CA), Polaris optical tracking system (NDI, Waterloo, Canada), Imaging and surgical navigation platform—TREK (I-STAR Lab, JHMI), skull phantom and pre-operative CT images.

### **2.1C-arm Cone Beam CT imaging device**

A mobile C-arm for intra-operative CBCT has been developed in collaboration with Siemens Healthcare (Siemens SP, Erlangen Germany). The main modifications to the C-arm include replacement of the X-ray image intensifier with a large area FPD (PaxScan 4030CB, Varian Imaging Products, Palo Alto, CA) allowing a FOV of 20\*20\*15 cm<sup>3</sup> at the isocenter and soft-tissue imaging capability, motorization of the C-arm orbit and development of a geometric calibration method and integration with a computer-control system for image readout and 3D reconstruction by a modified Feldkamp algorithm. Applications under investigation range from image-guided brachytherapy to orthopedic and head and neck surgery.

Volume images are reconstructed from x-ray projections acquired over the C-arm orbit  $\sim 178^\circ$ , recognizing that the orbit less than  $180^\circ$  +fan angle imparts a limited-angle artifact as described previously. The FPD has  $2048 \times 1536$  pixels with a pitch of 0.194 mm, which is binned upon readout to  $1024 \times 768$  pixels dynamic gain readout, in which the gain of detector readout amplifiers scales dynamically with the pixel signal as a means of improving dynamic range and CBCT image quality. CBCT imaging entails acquisition of 100–500 projections reconstructed at 0.2–1.6 mm voxel size (depending on speed and image quality requirements)—nominally 200 projections reconstructed at 0.8 mm voxel size ( $256 \times 256 \times 192$  voxels). Filtered back projection is performed using a modified Feldkamp algorithm, with mechanical nonidealities of the C-arm accommodated using a geometric calibration. The resulting CBCT images demonstrate sub-mm 3D spatial resolution and soft tissue visibility. All images in this study were acquired at an imaging dose sufficient for both bony detail and soft-tissue visibility. Acquisition time was typically 60 s, and reconstruction on a PC workstation (Quad Core 2.8 GHz, 4 GB RAM, Dell, Round Rock, TX) takes 20 s [5].

### 2.2 NeuroMate skull base robot system

The NeuroMate robot (Integrated Surgical Systems, Sacramento, CA) is an FDA-cleared image-guided robotic system designed for stereotactic procedures in neurosurgery. The rationale for using this robot includes its mechanical stiffness, good accuracy and convenient workspace for cranial procedures. While the robot was originally designed for positioning and orientating surgical tools, it was converted the NeuroMate into a cooperatively-controlled robot by attaching a six-DoF force sensor (JR3 Inc., Woodland, CA, USA) at the end effector, between the final axis and the surgical instrument (Anspach eMax drill, Palm Beach Gardens, FL, USA). Forces and torques exerted by the surgeon are translated into joint motions to move the instrument in the direction of the applied force. The system can allow unimpeded



Fig 5: NeuroMate robot [2]

motion of the instrument or can impose ‘virtual fixtures’ to guide the surgeon’s hand and/or enforce safety constraints, as described in the section on Virtual fixture. The robot kinematic equations, including tool calibration, provide the location of the cutter tip relative to the Robot world frame [3].

### 2.3 Polaris optical tracking system

The IR tracking system (Polaris, NDI, Waterloo, ON) was used to measure the position of reflective spherical markers. According to the manufacturer specifications, the camera provides RMS accuracy of 0.25 mm in marker localization sufficient to encompass the imaging FOV of the C-arm. The markers were affixed to trackable tools (e.g., a pointer) or objects (e.g., the skull phantom or robot arm). A reference tool was used with the tracking system to ensure that perturbation of the camera or object



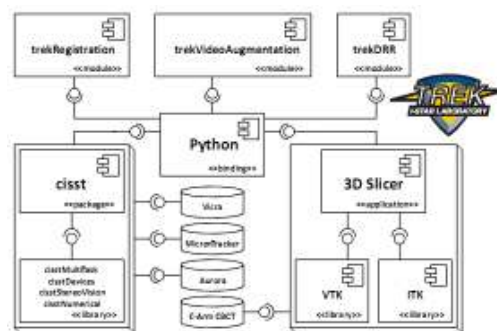
Fig 6: NDI Tracker

would not result in loss of registration. In our system, a passive probe is used to collect positions of fiducials on the surface of the phantom. One reference marker is attached near the skull phantom as the reference frame. Another reference marker is attached on the robot arm so that the position of robot cutter tip can be tracked in real-time [5]. (The picture shows above is from [http://4navitec.com/Products/Consulting/Characterization/body\\_characterization.html](http://4navitec.com/Products/Consulting/Characterization/body_characterization.html))

## 2.4 Imaging and surgical navigation platform—TREK

TREK is an imaging and surgical navigation platform for cone-beam CT guided surgery. It is founded on two major complementary software packages: the cisst libraries (Johns Hopkins University, Baltimore MD) for surgical navigation and the 3D Slicer application package (Brigham and Women's Hospital, Boston MA) for image visualization and analysis, each of which utilize other open-source software libraries such as VTK and ITK (KitWare, Clifton Park NY) [6].

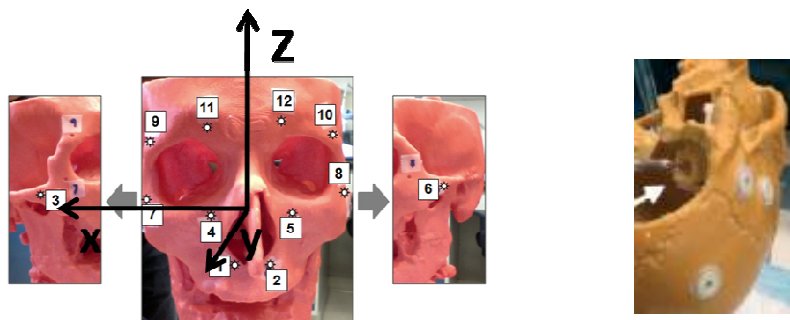
The surgical guidance system has modular software architecture—interface with a prototype mobile C-arm for high-quality CBCT and integration of different tools and devices consistent with surgical workflow. Specific modules related to this project are: compatibility with infrared, electromagnetic, and video-based trackers used individually or in hybrid arrangements; quantitative tools that analyze and communicate factors of geometric precision



including fiducial (FRE) and target registration error (TRE); 3D-3D rigid or deformable registration of preoperative images, surgical planning data, and up-to-date CBCT images [6].

## 2.5 Phantom

The phantom used in first part of this project, Red Skull, is made of Acrylonitrile Butadiene Styrene (ABS) and Polycarbonates (PC). It was originally designed to facilitate the development of tracking system for rigid/flexible endoscope and provide qualitative assessment of tracking system performance. Rapid prototype and 3D printing technology has been employed for the development of the phantom, allowing a high-precision and realistic anatomical structure to present in the phantom. Custom design of cone-shaped divot points and fiducial markers are introduced to the critical anatomical sites on the surface and inside the phantom respectively [7]. An illustration of the distribution of divot points is showed in Fig.



1 (left) [7] and foam phantom (right) [3]



The phantom used in second part of this project consists of a plastic skull with adhesive fiducials. A unique feature of this phantom is that it contains an embedded fixture for holding a precisely machined foam block. This custom design provides reliable fixture of foam block, preventing any movement during drilling.

## 3 Methods

### 3.1 Overview of registration workflow

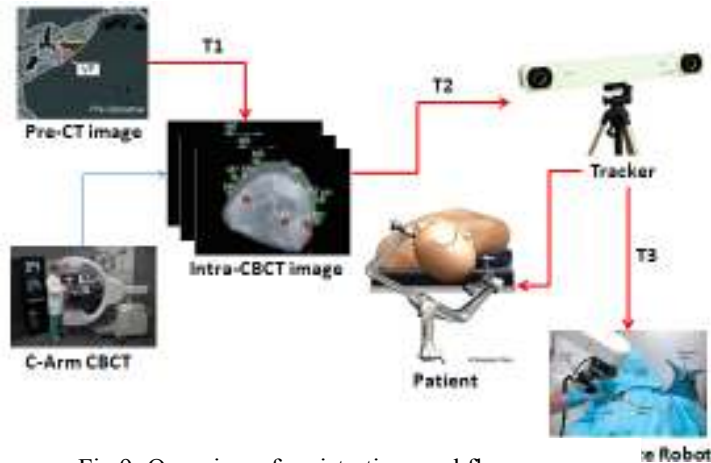


Fig 9: Overview of registration workflow

The diagram shows the registration workflow of this system, which includes a series of 3D-3D registration. The first registration between pre-operative CT images to intra-operative CBCT images is designed to transform virtual fixture defined in CT coordinate to CBCT coordinate. The second one between intra-operative CBCT coordinate and tracker coordinate is a typical image-to-world registration. The third one between robot world frame and tracker coordinate is used to integrate robot system to current navigation system. If all the registrations above are achieved, the virtual fixture can be transformed all the way down to robot world frame and perform constrain directly in the robot world frame. Also, the position of robot cutter tip can be tracked and visualized in real time in the navigation system.

### 3.2 Technical approach

- Pre-operation
  - Obtain CT Image of patient head
  - Create virtual fixture on CT image in TREK
- Right before operation
  - Obtain CBCT Image of patient head
  - CBCT to CT registration
    - ◆ Pick up fiducials in both CBCT and CT images in TREK
    - ◆ Paired-point registration
  - CBCT to tracker registration
    - ◆ Use passive probe to point fiducials on patient head
    - ◆ Paired-point registration



- Robot to Dynamic Reference Base (relative to tracker)registration (Dynamic Reference Base is mounted on the head clamp)
  - ◆ Get tip position with reference to Robot World frame
    - Do pivot calibration to get cutter tip position with reference to Tool Center Point frame
    - Calculate tip position with reference to Robot World frame using forward kinematics
  - ◆ Get tip position with reference to DRB frame
    - Attach rigid body to robot cutting tool
    - Do pivot calibration to get cutter tip position with reference to robot rigid body frame
    - Calculate tip position with reference to DRB frame using navigation system
  - ◆ Paired-point registration
- Register virtual fixture from CT image frame to Robot World frame using the transformation flow above, prevent tool from entering “no-fly-zone”
- Intra-operation
  - A neurosurgeon holds the robotic arm and drills in cooperatively controlled fashion guided by CBCT image and navigation system and protected by virtual fixture
  - Obtain CBCT images after achieving each milestone in surgery
  - Register new CBCT image to earlier ones, update deformation information and virtual fixture
- Post-operation
  - A CBCT image is taken to evaluate the operation results

## 4. Experiments and Results

### 4.1 Experiment methods

To fit Cone Beam CT imaging device into current robot system and design a reliable workflow for the new integrated system, we worked out how to setup and make use of a series of software tools and created some interface and GUI.

In specific, we worked out and documented how to

- (1) compile TREK on Windows, write TREK configuration file, use TREK for 3D-3D image registration, image-to-world registration, FRE and TRE measurement, virtual fixture generation
- (2) compile cisst libraries with Qt both on Windows and Linux
- (3) use NDI Track software for tracking and calibration
- (4) use robot program to calibrate drill, register robot to tracker and guide robot in comply mode
- (5) use VFCreator to modify virtual fixture and generate txt file
- (6) fix robot joints once broken

We also

- (1) created interface between NDI Tracker and robot program via devNDISerial class, so that NDI data can be transported into robot program in real time

- (2) designed GUI in robot program using FLTK and Qt Creator, to real time display NDI data
- (3) created interface between TREK and robot program via OpenIGTLinks

**4.1.1 Pre-operative CT to intra-operative CBCT registration**

We start this 3D-3D registration with rigid method, which considers the transform as three dimensional rotation and translation. The rigid method is very fast and accurate enough while it does not take deformation into consideration. In the clinical scenario, this registration is performed after the first CBCT image is taken when the patient’s head is fixed to the head clamp. One more thing to mention is that, during operation, another several CBCT scans may be performed and registered with former CBCT images by a 3D-3D registration similar to the method described here.



Fig 10: Fiducials in CBCT (left) [5] and CT (right)

First, a set of fiducials on the surface of the patient’s head both visible in CT and CBCT images are segmented in ‘Fiducial’ module in TREK (also in 3D Slicer). Then, a paired-point registration algorithm is performed in ‘FiducialRegistration’ module in TREK (also in 3D Slicer) and output a 4 by 4 matrix containing both rotation and translation. A feature in TREK not in 3D Slicer is that, in its ‘VideoAugmentation’ module, quantitative measurement of registration results such as fiducial (FRE) and target registration error (TRE) can be done automatically and displayed on screen after assigning fiducial and target points. In this way, an optimal fiducial point configuration can be selected after comparing FRE and TRE, and the final transform will be generated.

We set this rigid method as basic deliverable of our project. In future, the result of this rigid method will be used as an initial for more advanced image-based deformable registration. A possible solution is Demons registration with intensity matching [8].

**4.1.2 Image to tracker registration**

This registration is performed also in ‘VideoAugmentation’ module in TREK. A serial port cable connects NDI Polaris and a workstation with TREK installed and transport real time data from Polaris to TREK. The transform in this step is an affine transform containing three dimensional rotation and translation.

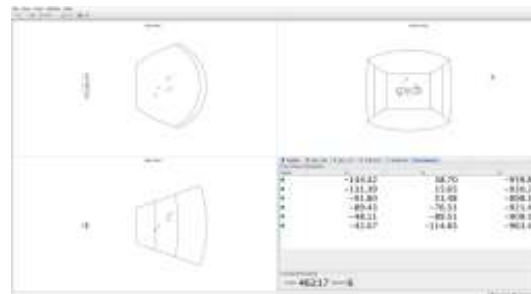


Fig 11 ‘Track’ software GUI

Before registration, the NDI passive probe needs to be calibrated in a NDI software named ‘Track’ to get the offset (a three dimensional vector). The offset then needs to be written into the configuration file of TREK.

During registration, first, a person points a NDI passive probe to a fiducial on the patient’s head and adjusts the orientation of the pointer until all the markers on the pointer are in the field of view of the Polaris. Then, he/she clicks the ‘capture’ button in the ‘VideoAugmentation’ GUI to finish locating a fiducial. These two steps are performed several times to obtain a list of fiducials. If one fiducial is not captured successfully into TREK or introduces too much error, it can be re-captured again and again until satisfaction. Note that the order of fiducials to capture should be the same as that of segmented fiducials. After selecting a subset of fiducials among all the captured ones, a paired-point registration algorithm will be performed and output an affine transform. One can also try different configuration of fiducials and choose the optimal one.

### 4.1.3 Robot to tracker registration

#### 4.1.3.1 Interface between NDI Tracker to robot program

As the StealthStation® is not functioning, we directly use NDI tracker to construct our own navigation system. The following figure is the control and information GUI for the NDI Tracker.



Fig 12: NDI Tracker GUI

All the components are connected and controlled by a periodic Control Task. Previously, the StealthStation® was connected to Control Task using StealthLink interface. As we now use the NDI tracker to substitute the StealthStation®, the StealthLink interface is no longer useful. So a new Control interface is designed for controlling the NDI tracker such as initializing and starting tracking task and a new Tool interface is used for data transfer.

The previous system separates Main Task and Control Task. This is a fairly good design, which allows us to keep using the same interface between Main Task and Control Task and also do not need to change the code in Main Task. So, what we do is modifying the code related to StealthStation in Control Task in order to receive data directly from NDI tracker, at the same time, still use the previous interface to communicate with Main Task. To implement this idea, we use devNDISerial class in cisst libraries (Johns Hopkins University) and modify some data type libraries to support data type conversion between StealthStation® and NDI Tracker.

The final test shows that the new interface using devNDISerial transports data accurately and fast. The new GUI responds to user commands and display location information correctly.

#### 4.1.3.2 Pivot Calibration

Pivot calibration can be used to get tooltip offset. In the robot to tracker registration process, there are 2 offsets, one in robot end effector frame and another in Robot Rigid Body frame.

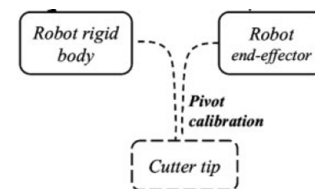


Fig 13: Pivot calibration [3]

Pivot calibration in robot end effector frame: ball-in-cone method.

First, the robot is guided to a far point and a near point. It will then compute the axis defined by these two points and move along the axis with the direction from far

point to near point. Once reaching the edge of a divot, it will compare the sensed force with the applied force. Ideally, when the tool tip is at the bottom of the divot, the sensed force will be equal to the applied force. In practice, we assign a tolerance (as seen in fig) for the difference between two forces. This ball-in-cone method is performed 6 times with difference robot gestures each time.

Pivot calibration in robot rigid body frame: Since a robot tool attached with a rigid body can be regarded as a passive probe in calibration, we remove the ablation tool from the robot and perform a typical offset calibration in software 'Track' as we do for the passive probe before.

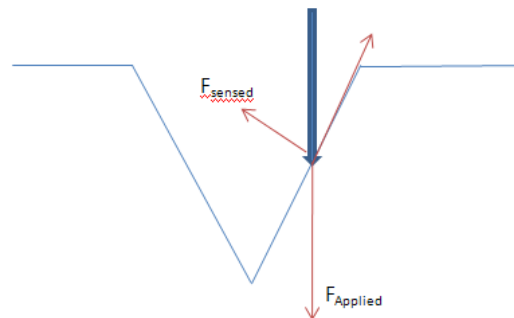


Fig 14: Ball-in-cone method

#### 4.1.4 Virtual Fixture

To generate a virtual fixture, we use 3D Slicer to generate a surface model from the pre-operative images and segment a region of interest (e.g. a VTK polydata file). We simplify the model by creating a six-sided convex hull and removing one or two sides to enable cutter entry in self-made software named VFCreator in Prof. Peter Kazanzides' lab. Justification for the simplification is based on clinical input that a 'box-like' virtual fixture is sufficient for many skull-base procedures, such as the suboccipital approach for acoustic neuroma resection, as simulated in our phantom experiments [3].

The details about the virtual fixture algorithm can be seen in [3]. Generally speaking, the workspace of the robot is divided into three regions: 1. A safe zone in which the robot is free to move. 2. A boundary zone between the safe region and the forbidden region. Here, motion of the robot may be restricted, as described below. 3. The forbidden region, which the cutting tool should not penetrate.

#### 4.1.5 Real time visualization of cutting tool

We also use 3D Slicer for intra-operative visualization of the cutting tool with respect to the intra-operative CBCT images. The robot software provides periodic updates of tool position and orientation to 3D Slicer via a network interface called OpenIGTLink (NAMIC). In specific, we set 3D Slicer as server in its 'OpenIGTLink' module and give its IP address to the robot program, which is set as a client. The OpenIGT function is added in control level of the robot program. Since the robot program continuously receives updated location of the cutter tip from NDI Tracker, the OpenIGT function can continuously send this information to 3D Slicer for display purpose.

#### 4.1.6 Summary of system integration

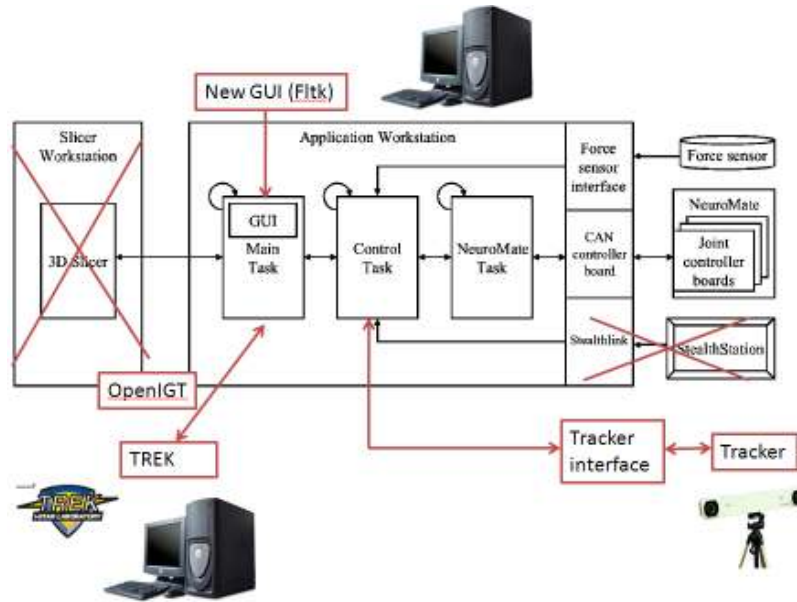


Fig 15: System Integration

#### 4.2 Experiment results on Red Skull phantom

This is the first series of experiments which have been done on Red Skull phantom in order to test the workflow and performance of each registration step.

##### 4.2.1 Pre-operative CT to intra-operative CBCT registration

We start from fiducial based registration. Eight fiducials are segmented both in CT and CBCT images. Except for the condition that all the selected fiducials fall into the same plane, under different fiducial configurations, the mean Fiducial registration error (FRE) is around 0.8 mm (smaller than 1mm) and the mean target registration error (TRE) is around 1mm. This result indicates this registration step achieves sub-millimeter accuracy and is acceptable.

Take a typical set of configuration as an example. 4 fiducials are selected among the 8 candidates as fiducial points, 2 fiducials are selected as target points, and 2 fiducials are discarded due to large error. The mean FRE is 0.86 mm (0.75 mm, 1.20 mm, 0.55 mm, 0.93 mm) and the mean TRE is 0.84 mm (0.85mm, 0.83mm).

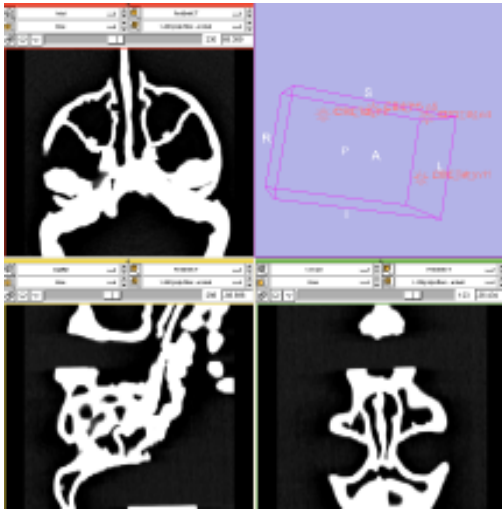


Fig 16: Pre-opera CT images

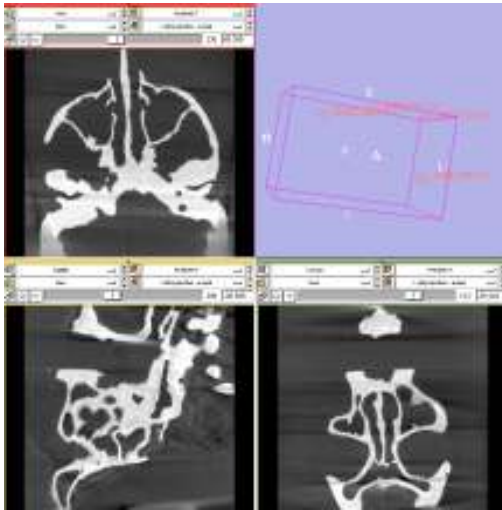


Fig 17: Intra-opera CBCT images

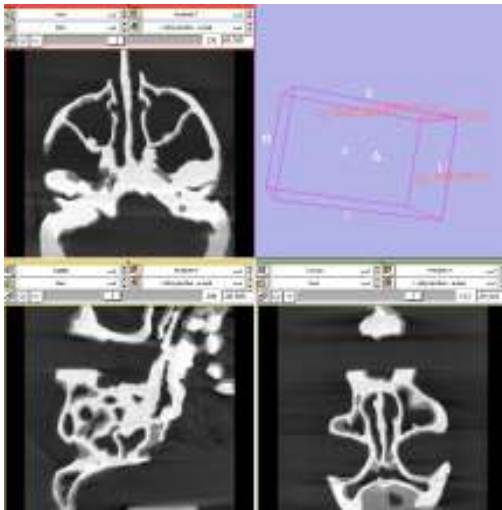


Fig 18: Overlay of CT and CBCT images

We also tried image based registration using registration module in 3D Slicer but it did not work well. This may be due to the difference in intensity pattern between CT and CBCT images. A possible solution is to introduce advanced processing like intensity matching.

#### 4.2.2 CT to tracker registration

The method is described in 4.1.2 and the scenario is shown in fig.... The passive probe we use here is a typical NDI passive probe (tool definition file: 8700339.rom). 8 fiducial points are located by NDI Tracker and transported into TREK. Some fiducials are not located accurately because they are partially out of view to NDI Tracker. Under different fiducial configurations, the mean Fiducial registration error (FRE) is between 0.5 mm to 0.8 mm and the mean target registration error (TRE) is below 1mm. This result also indicates this registration step achieves sub-millimeter accuracy and is acceptable. In addition, we find the repeatability of achieving high accuracy in this registration is fairly high, which indicates it is a highly reliable registration step.



Fig 19: CBCT-Tracker Registration

Take a typical set of configuration as an example. 5 fiducials are selected among the 8 candidates as fiducial points, 3 fiducials are selected as target points, and no fiducial is discarded due to large error. The mean FRE is 0.85 mm (0.71 mm, 0.55 mm, 0.20 mm, 1.83 mm, 0.98mm) and the mean TRE is 0.92 mm (0.43mm, 0.71mm, 1.62mm).

After registration, one can hold a passive probe and navigate towards the skull. The 3D layout of TREK is capable of real time displaying where the pointer tip is relative to the skull.

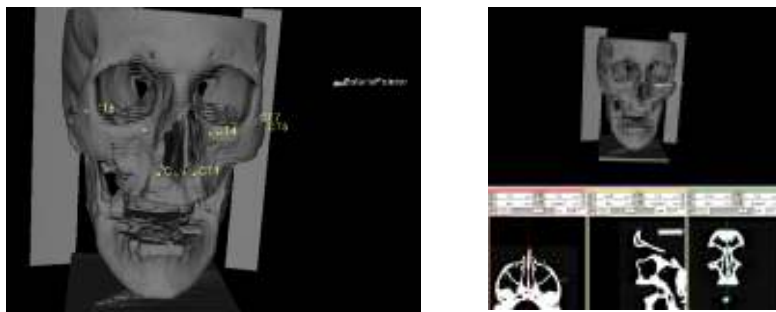


Fig 20: Slice views of the tracked pointer with respect to CT images

#### 4.2.3 Robot to tracker registration

In this part of the experiment, we concentrate on testing the performance of two features: 1) newly designed interface between NDI tracker and robot program and 2) Ball in Cone Search Method for robot pivot calibration. The scenario is shown in fig...



For the former feature, the robot program is now capable of displaying locations of both pointer and reference at the same time, just as the commercial software 'Track' does. For the latter one, we find at first it difficult to always properly guide the robot to different positions. With accumulated knowledge of how to use translation and rotation to guide robot in comply mode and avoid singularities, we finally succeed in performing this bone in cone search method 6 times and obtain an offset of robot cutter tip with low residual error.



Fig 20: Robot-Tracker Registration

### 4.3 Experiment results on foam phantom

#### 4.3.1 A robot tool for ablation

A typical clinical application of this skull base robot is to drill a certain area of bone in the patient head, as demonstrated in [3]. However, drilling foam in phantom experiment will produce messiness, which should be inhibited in mock room where the robot currently sits. As an alternative solution, we mount a soldering iron on the robot arm to make it a tool for ablating foam. Pre-experiment shows foam ablation is a procedure that can be controlled as slowly and precisely as foam drilling while do not produce messiness in the air.



Fig 21: Foam ablation tool

#### 4.3.2 Image to tracker registration

We performed the same registration method described in 4.1.2 and 4.2.2. The fiducials we use are five iron spheres attached on the surface of the phantom, which are more recognizable in CBCT than original fiducials on the phantom. One iron sphere is not in field of view in CBCT images so we use 4 iron spheres for registration. The mean FRE and TRE both achieve sub-millimeter accuracy as in 4.2.2 so that are acceptable. Currently we need to write the transformation matrix from CBCT image coordinate to dynamic reference body coordinate into a text file and load into robot program. In this experiment setup, an example of such file (NDIRegistrationResult.txt) looks like:

rotation -0.137779 -0.924697 -0.354899 -0.0963085 0.369126 -0.924376 0.98577 -0.0931796  
-0.139914 translation 102.095 67.7171 -168.571

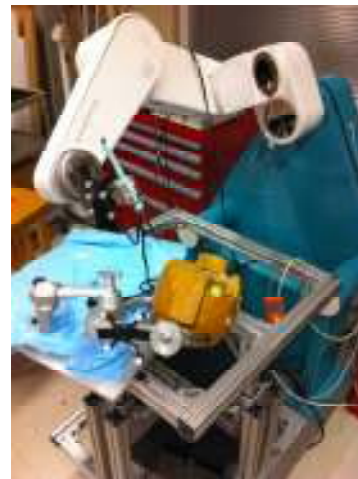


Fig 22: Experiment setup

### 4.3.3 Robot to tracker registration

The current setup of skull base robot system is shown in fig. The skull phantom is fixed by a head clamp which is then fixed to the robot base. The tool we design for ablation is mounted on the force sensor. A dynamic reference base (DRB) (tool definition file: 8700339.rom) and a robot rigid body (RRB) (tool definition file: 8700338.rom), both of which are products of Northern Digital Inc., are attached to the head clamp and robot tool, respectively. A NDI Polaris Tracker is placed around 1.5m away from the robot, facing the phantom area.

The first step is pivot calibration of the robot tool in both robot end effector frame and robot rigid body frame. The methods are described in details in 4.1.3.2. Both calibrations achieve high accuracy.

(1)Pivot calibration in robot end effector frame. The following is the result we choose as the tooltip offset for robot-to-tracker registration later.

Tool	Tip offset x	Tip offset y	Tip offset z	Residual Error
Soldering iron	161.261599 mm	-2.617605 mm	-163.316886 mm	0.433989 mm

(2)Pivot calibration in robot rigid body frame. We choose the result from Experiment 2 for robot-to-tracker registration later, because its RMS Error is lower and the Min Angle is above the required minimum 30°.

Experiment	Tip offset x	Tip offset y	Tip offset z	RMS Error	Min Angle
1	-28.33 mm	-22.72 mm	160.61 mm	0.70 mm	43.64°
2	-29.46 mm	-22.10 mm	160.41 mm	0.57 mm	38.61°

The second step is robot-to-tracker registration. The robot tooltip is guided to six different positions, which are recorded in both robot world frame and Polaris tracker frame. Then, a paired-point registration algorithm is performed and output the transform between robot world frame and dynamic reference body frame. The following is the output transformation matrix. The residual error is 0.646216 mm, which is good and acceptable compared with previous studies [3].

0.035234	0.998668	-0.037698	-634.418109
-0.813642	0.050568	0.579163	-49.076551
0.580298	0.010266	0.814340	-193.520591
0	0	0	1

### 4.3.4 Target-pointing experiment results

We validate the registration accuracy of the whole system in two methods: target-pointing and virtual fixture. In the first one, we pick a fiducial point A in CBCT images (P\_Fid1\_CBCT), and use the two transforms, CBCT-to-tracker (F\_Reference\_CBCT) and robot-to-tracker (F\_Reference\_Robot), which are the registration results above, to compute an estimated location in robot world frame (P\_Fid1\_Robot\_Estimate).

$$P\_Fid1\_Robot\_Estimate = inv(F\_Reference\_Robot) * F\_Reference\_CBCT * P\_Fid1\_CBCT;$$

Then we guide the robot to fiducial point A on the phantom in real world and read its position in robot world frame (truth, P\_Fid1\_Robot\_Truth) from robot GUI. We define error as subtraction of

the estimated position and the truth.

**Fiducial Point A**

	Fid1 in CBCT	Fid1 in Robot world (Estimate)	Fid1 in Robot world (Truth)	Error(Absolute)
X	-48.38 mm	-230.09 mm	-230.83 mm	0.74 mm
Y	50.27 mm	625.73 mm	625.60 mm	0.13 mm
Z	-18.80 mm	-192.18 mm	-190.86 mm	1.32 mm

**Fiducial Point B**

	Fid2 in CBCT	Fid2 in Robot world (Estimate)	Fid1 in Robot world (Truth)	Error(Absolute)
X	-49.06 mm	-192.32 mm	-191.72 mm	0.60 mm
Y	36.62 mm	554.53 mm	555.55 mm	1.02 mm
Z	63.58 mm	-214.07 mm	-215.76 mm	1.69 mm

The results show the whole system achieves sub-millimeter registration accuracy in x and y dimensions, reaching the same level of accuracy as in previous studies [3]. However, in z dimension, the registration accuracy is a little lower than previous studies reported in [3].

A possible reason is that some joints of the robot may have accumulated offsets larger than before and have not been calibrated. In future, we plan to calibrate the robot in this way: measure the horizontality or verticality of each joint when its angle is set to zero. Another possible reason for the larger error in z dimension is that manual segmentation of fiducial A and B may have introduced larger error in that dimension than x and y dimension.

**4.3.5 Virtual fixture experiment results**

We generate a virtual fixture with the shape of six-sided convex hull in 3D Slicer as described in 4.1.4. The convex hull is within the foam as seen from the three slices.

We then loaded the virtual fixture (vtk file) into software VFCreator mentioned in 4.1.4 and deleted one side from the six sides in order to let robot enter this convex hull. The output of this software is a text file containing definitions of the five sides as shown below. The first three values are x, y, z value of the position of a point in that plane. The last three are x, y, z value of the normal vector of that point. All units are millimeter.

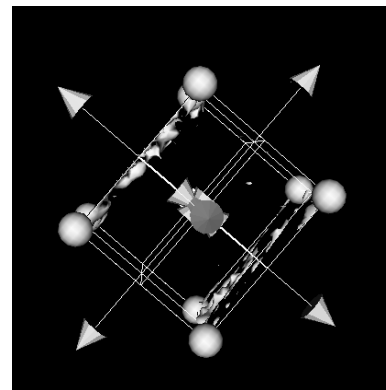


Fig 23: Virtual fixture

Plane	Position X	Position Y	Position Z	Normal X	Normal Y	Normal Z
1	25.000	-46.000	-4.000	-1.000000	-0.000000	-0.000000
2	15.000	-46.000	5.000	1.000000	-0.000000	-0.000000
3	15.000	-46.000	-4.000	-0.000000	-1.000000	-0.000000
4	25.000	-57.000	-4.000	-0.000000	1.000000	-0.000000
5	25.000	-46.000	-4.000	-0.000000	-0.000000	1.000000

Next, we load the virtual fixture into robot program and the program automatically transforms the virtual fixture from CBCT image coordinate into robot world coordinate. The transformation equation is exactly the same as shown in the target-pointing experiment in 4.3.4. This again indicates the importance of performing target-pointing experiment before virtual fixture experiment.

The most important step is guiding the robot to ablate within the virtual fixture. As described in 4.1.5, we use OpenIGTLink to real-time visualize the position of the robot tool tip in CBCT image (left figure). Also, once loading the virtual fixture into the scene, we can also visually check whether the robot tool tip is inside the virtual fixture or not. We believe this is also an important function in clinics where a surgeon is able to monitor the safety of the procedure using his/her own eyes.

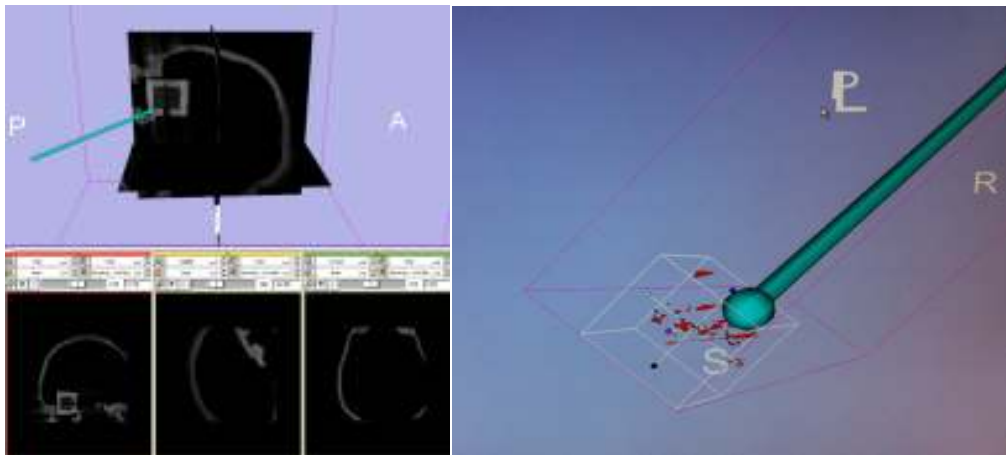


Fig 24: Real time visualization of tool tip

The images shown in fig are intra-operative CBCT images of the ablated foam, which demonstrate both the feasibility of integrating CBCT imaging into robot-assisted surgical procedures, and the effectiveness of virtual fixture in constraining the ablation. During the ablation, we could physically sense the resistance virtual fixture brings to us when we want to move the robot tool tip away from the target area. In future, we plan to quantitatively measure the ablation outcome, e.g. placement and dimensional error [3]. We also plan to generate and perform experiment on more kinds of virtual fixture to examine the advantages and disadvantages of current virtual fixture method.

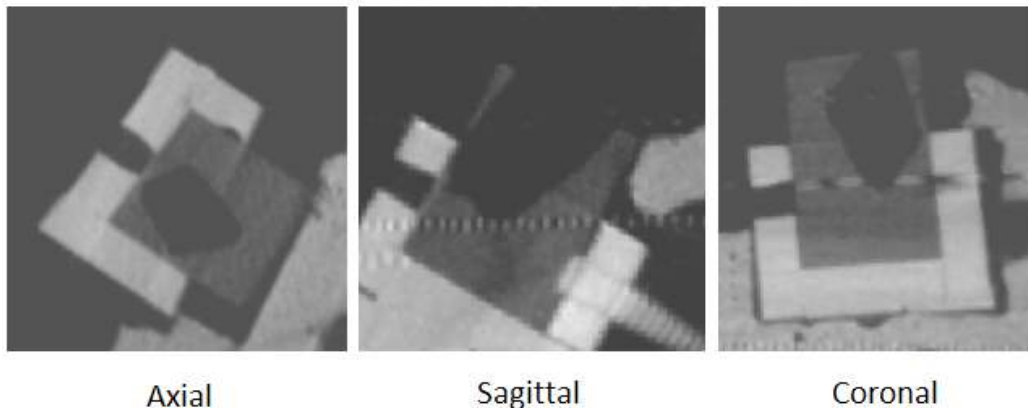


Fig 25: Intra-operative CBCT images of ablated foam

## **5 Management summaries**

### **5.1 Credits**

Hao is a graduate student in BME (Biomedical Engineering) and has background in medical imaging and image registration. So, he has accomplished most of the work on CT-CBCT registration, CBCT-Tracker registration, setup and use of navigation system TREK, segmentation of surface model for virtual fixture generation, coordination with C-arm Operator for CBCT scan.

Zihan is a graduate student in ME (Mechanical Engineering) and has background in robot control and kinematics. So, he has accomplished most of the work on Robot-Tracker registration, operating and repairing robot, and programming on system integration (building tracker-robot and TREK-robot interface).

Hao and Zihan work together on designing the registration workflow, setting up the whole system, and performing the two types of phantom experiments.

### **5.2 Accomplishment vs. Plan**

We have accomplished all minimum and expected deliverables as listed below. The only change is that we replaced foam drilling with foam ablation to avoid messiness in the Mock OR.

Minimum:

1. Fusion of intro-opera CBCT and pre-opera CT images by fiducial-based rigid registration
2. Complete transformation flow including robot, skull, CBCT images along with navigation system
3. Target-pointing experiment on phantom using CBCT-Guided skull base drilling robot system(CBR system) with navigation

Expected

1. Foam-drilling experiment on phantom using CGR system with navigation
2. Transformation flow including robot, skull, CBCT images without navigation
3. Parallel phantom experiments using two CGR systems and previous non-CBCT system. Compare results.

### **5.3 Future plan**

1. Quantitatively measure the ablation outcome, e.g. placement and dimensional error [3]. Also, generate and perform experiment on more kinds of virtual fixture to examine the advantages and disadvantages of current virtual fixture method.
2. Calibrate the robot joints by measuring the horizontality or verticality of each joint when its angle is set to zero.
3. Use intra-operative CBCT images to update certain registration during experiment, e.g. CBCT-CBCT and CBCT-Tracker registration. This will be very helpful if patient motion occurs. In addition, surgeons can navigate surgical tools on images with new update of bone resection and tissue deformation.
4. Cadaver experiments.

5. Replace fiducial-based rigid registration of CBCT and CT with image-based deformable registration. E.g. Demons deformable registration with intensity matching [8]

## 6 Technical appendices

### 6.1 How to use NDI software 'Track'

#### General steps

1. Connect NDI serial port cable to computer. Open software 'Track'.
2. Load wireless tool. For example, load 8700340.rom for the passive probe in C:\Program Files\Northern Digital Inc\Tool Definition Files
3. Put the tool in field of view and the system will start tracking.
4. Choose 'Report stray markers' to locate separate markers.

#### How to do pivot calibration on pointer and reference?

1. Make sure the software is displaying the tracking information of the tool you want to calibrate. Choose 'determine tool tip offset by pivoting the tool'.
2. Place the tool on a divot. Click on 'Start collection'. Repeat rotating the tool left and right, forward and backward as well as rotating along its axis.
3. Copy x, y, z to configuration file as offset if Root Mean Square error is below around 0.3.

#### How to write configuration files?

1. Set name and parameters for each tracker in 'trackers' section. Serial number can be found by right clicking on each tracking display window in software 'Track'. Pay attention to the correspondence of serial number and definition.
2. Set a series of name-reference correspondence in 'frames' section
3. In 'modules' section, set directory as the directory of this configuration file. Set scene if you want to load a scene automatically after loading this configuration file

### 6.2 How to install Qt on Windows/Linux

#### Windows

1. Download Qt libraries 4.7.2 for Windows (VS 2008, 218 MB) from <http://qt.nokia.com/downloads/windows-cpp-vs2008>
2. Install
3. In cmake, set CISST\_HAS\_QT and configure with Visual Studio 9
4. Set correct directory for QT\_QMAKE\_EXECUTABLE. This qmake.exe file is in the 'bin' folder under your installation directory of Qt. E.g. C:/Qt/bin/qmake.exe
5. Configure again. If qmake.exe is found by cmake, it will set all the other qt-related directories
6. Generate and build

#### Linux

1. Download Qt libraries 4.7.2 for Linux (VS 2008, 218 MB) from <http://qt.nokia.com/downloads/linux-x11-cpp>
2. Follow steps in <http://doc.qt.nokia.com/4.7/install-x11.html>

## 6.3 How to use software TREK

### Install on windows

1. Checkout source code from <https://svn.lcsr.jhu.edu/istar/trunk/trek>
2. Use cmake to configure and generate codes (see details on <https://trac.lcsr.jhu.edu/istar/wiki/trek>)
3. In DOS, type 'trek.bat build' to build (keep internet available).  
\* The workstation RedShift requires a second build. Cisstvsvars.bat was not created after first build.
4. Type 'trek.bat run' to run.

### Image-to-world registration

1. Load configuration file. e.g. Configuration.xml in D:\data\20110304\_Polaris
  2. Go to trekVideoAugmentation module
  3. Load a series of data includes CT image, CT model, and CT Fiducial list.
    - File -- Add Data – Apply (Data Centered)
    - Module: Choose Fiducials Module to create fid list and add fiducials
    - Fiducials Module: Can Choose View Model// Toolbar
    - RAS(d,d,d) is the location of a fiducial // Footbar
- \* Do not need this step if a scene has been set in configuration file.
4. Set 'Pointer Tool' to 'PolarisPointer'(for example), 'Reference Tool' to 'PolarisReference', 'Fixed Fiducials' to 'CTFids', 'Moving Fiducials' to 'create new fiducial list' such as 'PolarisFids'.
  5. Fix Polaris reference on the phantom's head. Make sure the head will not move.
  6. Choose 'Start/stop'.
  7. Place the Polaris pointer to fiducial No.1 and click on 'capture fiducial'.
  8. Repeat step 7 for several fiducials. If registration error of a certain fiducial is higher than accepted, repeat step 7 on this fiducial.
- \* It is recommended to cover fiducials in different parts of the head to make registration more reliable.

### Real-time Tracking

1. Set 'Frame Actor' as 'Axes' or 'Cone', set 'slicing' to 'orthogonal', set 'slice field of view' to zoom in and zoom out in slices.
2. Choose 'data' module to navigate on model (if there is) instead of slices.

### Image to image registration

Use fiducial registration module

Other documentations have been written but not included in this report (for privacy)

1. How to use NeuroMate
2. How to link neuromate and slices
3. How to do pivot calibration, how to register robot to tracker
4. How to generate VF
5. How to use VFCreator



## 7. References

- [1] <http://en.wikipedia.org/wiki/Neurosurgery>
- [2] Accuracy Improvement of a Neurosurgical Robot System
- [3] An integrated system for planning, navigation and robotic assistance for skull base surgery
- [4] [http://en.wikipedia.org/wiki/Computer\\_Integrated\\_Surgery](http://en.wikipedia.org/wiki/Computer_Integrated_Surgery)
- [5] Automatic image-to-world registration based on x-ray projections in cone-beam CT-guided interventions
- [6] Uneri A, Schafer S, Mirotta D, Nithiananthan S, Otake Y, Reaungamornrat S, Yoo J, Stayman JW, Reh D, Gallia GL, Khanna AJ, Hager G, Taylor RH, Kleinszig G, and Siewerdsen JH, "Architecture of a High-Performance Surgical Guidance System Based on C-Arm Cone-Beam CT: Software Platform for Technical Integration and Clinical Translation," SPIE Medical Imaging 2011: Visualization, Image-Guided Procedures, and Display Volume 7964: in press (2011).
- [7] An innovative phantom base on 3D printing technology for advanced endoscopic tracking system
- [8] Nithiananthan S, Schafer S, Uneri A, Mirotta DJ, Stayman JW, Zbijewski W, Brock KK, Daly MJ, Chan H, Irish JC, and Siewerdsen JH, "Demos deformable registration of CT and cone-beam CT using an iterative intensity matching approach," Med. Phys. 38(4): 1785 - 1798 (2011).
- [9] Siewerdsen JH, Moseley DJ, Burch S., Bisland S, Bogaards A, Wilson BA, and Jaffray DA, "Volume CT with a flat-panel detector on a mobile, isocentric C-arm: Pre-clinical investigation in guidance of minimally invasive surgery," Med. Phys. 32(1): 241-254 (2005).
- [10] C-arm Focus Group Agenda, Jan 2010